Analyst

PAPER

View Article Online
View Journal | View Issue

Cite this: *Analyst*, 2014, **139**, 5451

Incorporation of ^{57}Fe-isotopically enriched in apoferritin: formation and characterization of isotopically enriched Fe nanoparticles for metabolic studies†

T. Konz, M. Montes-Bayón* and A. Sanz-Medel*

The use of ^{57}Fe-isotopically enriched ferritin for the accurate measurement of Fe : ferritin ratios is proposed for metabolic studies. Thus, the synthesis of ^{57}Fe-isotopically enriched ferritin from horse apo-ferritin and isotopically enriched $(NH_4)_2{}^{57}Fe(II)(SO_4)_2$ (Mohr's salt) is conducted. Size exclusion chromatography on-line with UV-VIS absorption (at 380 nm) is used in order to monitor the loading process of apo-ferritin. These studies revealed that the Fe-incorporation process involves also the formation of protein aggregates (oligomers) showing higher molecular mass than ferritin. A final optimized protocol involving incubation of the synthesized standard with guanidine hydrochloride (pH 3.5) has provided the best conditions for maintaining a stable protein structure without aggregates. Such ^{57}Fe-isotopically enriched ferritin was characterized and contained an average of 2200 atoms of Fe per mole of ferritin. The evaluation of the Fe-core after saturation with ^{57}Fe by Transmission Electron Microscopy (TEM) has revealed the formation of ^{57}Fe nanoparticles with a similar diameter to that of the commercial Fe-containing ferritin, confirming the process of Fe uptake, oxidation and mineralization within the protein cavity. The synthesized ^{57}Fe-ferritin shows great potential as a nanometabolic tracer to study the kinetics of Fe release in the cases of iron metabolic disorders.

Received 2nd July 2014
Accepted 4th August 2014

DOI: 10.1039/c4an01187b

www.rsc.org/analyst

Introduction

Iron is an essential micronutrient that is required for an adequate erythropoietic function, oxidative metabolism and cellular immune response.[1] Absorption of dietary iron (1–2 mg per day) is tightly regulated, and balanced with losses, because there is no active mechanism of iron excretion.[2] The measurement of iron imbalances in organisms includes a number of parameters related to the main iron transporting protein in plasma, transferrin (Tf).[3] Among them, the Tf-saturation level (amount of Fe associated with Tf binding sites) or serum iron is commonly monitored in clinical labs.[4,5] In addition to Tf-related parameters, ferritin is the other key biomarker in Fe metabolism.[6,7] Actually, the measurement of ferritin provides the most useful indirect estimation of body iron stores.[8]

Ferritin is a 440 kDa protein composed of 24 subunits that form a hollow protein shell holding inside an internal cavity of about 8 nm internal diameter that can contain a variable amount of iron atoms (up to 4500) by forming so-called biological nanoparticles.[9,10] The 24 polypeptide subunits do not have the same structure and function. While the H-chain (21 kDa) shows catalytic ferroxidase activity and is responsible for the oxidation of Fe(II) to Fe(II), the L-subunit (19 kDa) is associated with iron nucleation, mineralization and long-term iron storage within the ferritin cavity mainly in the form of Fe_2O_3 nanoparticles (NPs).[11] The chain H/L ratio varies among tissues and therefore, the number of Fe atoms stored into the internal cavity of ferritin is not constant either.[12] In fact, the Fe load of ferritin has been proposed by some authors as a more specific biomarker of Fe-homeostasis disorders than the measurement of only the protein shell. Nowadays, ferritin (and its Fe content) is increasingly being recognized as a crucial molecule in some neurological pathologies such as Parkinson (PD) or Alzheimer's (AD) diseases. In PD patients a marked reduction of the ferritin expression in the brain as well as the alteration of the neuromelanin structure seems to compromise the iron sequestration capabilities leading to the accumulation of free metal ions. Thus, understanding the chemical structure of the ferritin core may help to elucidate the alteration or dysfunction of ferritin and its role in the development of degenerative diseases. This includes the ferritin iron uptake, storage, and release mechanisms in detail in order to understand the etiologic origin of some of these syndromes.[13,14]

For the aim of studying Fe-ferritin related parameters an interesting possibility is the use of ^{57}Fe-isotopically enriched

Department of Physical and Analytical Chemistry, Faculty of Chemistry, University of Oviedo, C/Julián Clavería 8, 33006 Oviedo, Spain. E-mail: montesmaria@uniovi.es; asm@uniovi.es

† Electronic supplementary information (ESI) available. See DOI: 10.1039/c4an01187b

ferritin. Using a non-toxic isotopic label is especially favourable to investigate, among others, whether serum ferritin losses most of its Fe during or after effluxing from the cells in which it originates.[15] The synthesis and characterization of ^{57}Fe-ferritin have been attempted before by biochemical heterologous expression in *E. coli* in the presence of ^{57}Fe.[16,17] In this case, the expressed protein was the plant ferritin (different to the human species) and the production yield turned out to be relatively low. In this work, this challenging task has been accomplished by chemical synthesis using apo-ferritin from horse spleen that was then enriched in ^{57}Fe using isotopically enriched $(NH_4)_2{}^{57}Fe(II)(SO_4)_2$ (Mohr's salt), as the source of enriched Fe(II) previously synthesized. Different salts have been used in previous experiments for Fe-loading into apoferritin including $FeSO_4$ or $(NH_4)_2Fe(SO_4)_2$. This double sulphate (Mohr's salt) has been chosen since Fe(II) present in the compound is less prone to be oxidized by the dissolved oxygen than other Fe(II) salts. The oxidation of Fe(II) is very pH dependent, occurring much more readily at high pH. The ammonium ions make solutions of Mohr's salt slightly acidic, which slows this oxidation process. Both the ^{57}Fe incorporation kinetics and the stability of the synthesized metalloprotein have been carefully evaluated here. The final isotopically enriched protein has been quantitatively characterized for the metal (Fe) and the protein (S) using SEC-ICP-MS and post-column isotope dilution of sulphur and of iron (using enriched ^{34}S to address the protein content and reversed IDA with natural Fe to address the incorporated ^{57}Fe respectively).

The complementary information provided by TEM (monitoring the formation of iron NPs from isotopically enriched ^{57}Fe) together with the information obtained by SEC-ICP-MS (in terms of Fe isotope ratios and Fe/S measurements) has permitted to fully characterize the synthesized nanometabolic tracer ^{57}Fe-ferritin that shows extraordinary potential to address Fe/ferritin ratios in biological samples as well as kinetics studies on the iron mobilization mechanisms (*e.g.* in Alzheimer's disease).

Materials and methods

Instrumentation

All ICP-MS experiments during this study were performed using a Thermo Element 2 (Thermo Fisher Scientific, Bremen, Germany) mass spectrometer, equipped with a double focusing sector field mass analyzer applying medium resolution ($m/\Delta m = 4000$) both for Fe and S detection. The observed optimized parameters for Fe and S of the Element 2 instrument are summarized in Table 1. The ICP-MS instrument was fitted with a concentric nebulizer and a Scott double-pass spray chamber. For the final evaluation of ferritin purity, after its isolation from other serum components, we used size exclusion chromatography (SEC). HPLC separation was carried out using a dual-piston liquid chromatographic pump (Shimadzu LC-20AD, Shimadzu Corporation, Kyoto, Japan) equipped with a sample injection valve from Rheodyne, fitted with a 100 μL injection loop and a size exclusion chromatography column Superdex 200 10/300 GL (300 mm × 10 mm i.d., GE Healthcare Bio-Sciences, Sweden). The mobile phase flow was 0.75 mL min^{-1} and the absorbance of the ferritin was monitored at 280 and 380 nm (specific of the iron–protein complex) using a Diode Array Detector (DAD) (Agilent Technologies, Waldbronn, Germany).

Table 1 Instrumental operating conditions for Fe and S measurement in ferritin

Thermo Element 2	
RF power	1350 W
Mass resolution R	4000 (Medium resolution)
Isotopes monitored	^{56}Fe, ^{57}Fe, ^{32}S, ^{34}S
Nebulizer	Concentric
Spray chamber	Scott-double pass, 21 °C
Cooling gas	15.5 L min^{-1}
Auxiliary gas	0.90 L min^{-1}
Samples gas	0.90 L min^{-1}
HPLC devices and parameters	
HPLC device for UV/Vis	Agilent 1100 series
HPLC device for ICP-MS	Shimadzu LC-20AD
Flow rate	0.75 mL min^{-1}
Mobile phase	50 mM ammonium acetate (pH 7.4)
Chromatographic column	Superdex 200 10/300 GL

For evaluation of isotopic abundances of the ^{57}Fe-ferritin, the size exclusion column was coupled on-line with a multi-collector (MC)-ICP-MS (Neptune, Thermo Fisher Scientific). The Neptune MC-ICP-MS is equipped with eight adjustable Faraday cups, one fixed central cup, and a secondary electron multiplier. To increase the sensitivity, the instrument is also equipped with a guard electrode that improves the ion-transmission efficiency and prevents the formation of secondary discharges. Iron isotope ratio measurements were performed using the medium resolution setting of the entrance slit. The system configuration for Fe measurements is similar to the one described in the literature.[18]

TEM measurements were done using a JEOL-JEM 2100F (200 kV) transmission electron microscope to image ferritin solutions deposited on Cu grids. The instrument also permits to obtain the elemental composition of the sample.

Chemicals and materials

All solutions were prepared using 18 MΩ cm^{-1} de-ionized water obtained using a Milli-Q system (Millipore, Bedford, MA, USA). Ferritin standards from equine spleen (apo and Fe-containing), human spleen and human liver were purchased from Sigma-Aldrich (St. Louis, MO, USA). Isotopically enriched ^{34}S (abundances: ^{34}S 99.91% and ^{32}S 0.09%) used for ICP-MS protein quantification by IDA was purchased from Euriso-top (Saint-Aubin Cedex, France). Isotopically enriched elemental iron with relative abundances 0.043% ^{54}Fe, 4.96% ^{56}Fe, 94.52% ^{57}Fe, and 0.47% ^{58}Fe was obtained from Spectrascan (Teknolab A.S. Dröbak, Norway). The synthesis of Mohr's salt $(NH_4)_2{}^{57}Fe(II)(SO_4)_2$ from the solid is detailed in the procedure section.

The mobile phase for SEC separation of ferritin synthesis products was 50 mM ammonium acetate (pH 7.4) from Sigma Aldrich. For decreasing oligomer formation during the

synthesis of isotopically enriched ferritin, solutions containing 0.06 M dithiothreitol (DTT) or 7 M guanidinium hydrochloride were prepared from the corresponding solid compounds obtained from Sigma. Concentrated H_2SO_4 and $(NH_4)_2SO_4$ were purchased from Merck (Merck, Darmstadt, Germany) and HEPES from Sigma Aldrich.

Synthesis of ^{57}Fe enriched Mohr's salt

The suitability of the synthesis procedure was first evaluated with natural Fe(II) and then, scaled down to be applied to the more expensive isotopically enriched ^{57}Fe(II) in the more stable form of ammonium iron(II) sulphate. For the synthesis of ammonium iron(II) sulfate (Mohr's salt), 50 mg (0.9 mmol) of elemental ^{57}Fe and 0.9 mL of 1 M H_2SO_4 were placed in a glass vial. The vial was sealed with a septum and the mixture was allowed to stand overnight so that iron was completely dissolved. Separately, 118 mg (0.9 mmol) of $(NH_4)_2SO_4$ were dissolved in 140 μL water. Both solutions were simultaneously preconcentrated by evaporation using a hot plate. Immediately, after initial crystallization was observed, both solutions were mixed together by using a syringe. The reaction mixture was allowed to stand at 4 °C overnight. The light green crystals were collected by vacuum filtration and washed with a few μLs ice cold water. Typically, a yield of 60% was obtained. For the characterization of the final product, the measurement of the melting point as well as the X-ray diffraction spectra were used (see ESI†).

Synthesis of ^{57}Fe-ferritin from Mohr's salt and apoferritin

The loading of apo-ferritin with $(NH_4)_2{}^{57}Fe(II)(SO_4)_2$ was achieved by a modified protocol of the previously used by De Silva *et al.*[19] In brief, apo-ferritin was diluted in 50 mM HEPES buffer (pH 7.0) to give 4 mL of a 1 μM solution. Additionally, the incubation solution was prepared by dissolving 8 mg of ammonium iron(II) sulfate in 500 μL MilliQ-water to give a concentration of 40 mM. Apo-ferritin loading was achieved by adding 250 μL of the incubation solution to the 1 μM apo-ferritin solution (final Fe concentration approx. 2500 μM). The reaction mixture was allowed to stand for 30 min at room temperature. For the evaluation of the incorporation kinetics using $(NH_4)_2{}^{57}Fe(II)(SO_4)_2$ as a Fe(II) source, the absorbance of the Fe-protein complex was monitored at 380 nm using 1 μM apo-ferritin (fixed concentration) and concentrations of Fe(II) ranging from 0 to 10 mM. The absorbance was registered at different time intervals from 0 to 30 min.

To study the possible oligomerization events, after 30 minutes of incubation the solution was passed through a membrane filter with a 10 kDa cut-off to remove the Fe(II) excess (5000 *g*, 45 min, 4 °C) and the protein was washed several times with buffer 50 mM HEPES (pH 7). The product was then diluted in the mobile phase (50 mM ammonium acetate) and chromatographically analysed to address its evolution with time (1 h, 2 h, 3 h, 7 days and 14 days) in the absence of Fe and oxygen (N_2 was applied for degassing of the solution).

For the final cleavage of ferritin dimers and trimers, 1% DTT and 7 M guanidinium chloride were evaluated, as recommended elsewhere.[20] Optimum results were obtained by incubation of the residue obtained after ultracentrifugation with 4 mL of 7 M guanidinium chloride for 45 min. For further elimination of guanidinium chloride, the mixture was ultrafiltered again by using 10 kDa filters and washed twice with 50 mM HEPES buffer. The filter residue was finally dissolved in 4 mL of 50 mM ammonium acetate. Aliquots were stored at 4 °C. The purity of the ferritin solution was confirmed by size exclusion chromatography (SEC) and UV/Vis detection.

Quantification strategies used by isotope dilution analysis (IDA)

Quantitative analysis of the synthesized ^{57}Fe-ferritin was done by post-column isotope dilution using natural Fe and isotopically enriched ^{34}S simultaneously.[21–23] Ferritin recoveries through the SEC column were calculated to be 85% by Fe measurements. The accuracy of the determination of S by post-column IDA in the ferritin peak (as the mean to address the protein concentration) was validated by analysing a set of human liver commercial ferritin standards by this method and comparing results with a clinically used Ru-labelling immunoassay, as developed in previous studies.[24]

For quantification using species specific isotope dilution analysis, a fixed volume (100 μL) of the synthesized enriched ^{57}Fe-ferritin tracer (diluted to 6.68 μg Fe mL^{-1}) was mixed with equal volumes of the corresponding ferritin standards (apo and holo, with a theoretical concentration of 3.6 and 5.06 μg Fe mL^{-1}, respectively, according to the producer) and the mixture was injected in the SEC-ICP-MS system. These standards were quantified for total ferritin using the S content, by S post-column IDA.[21] By integrating the peak areas of ^{56}Fe and ^{57}Fe in the corresponding chromatograms and knowing the Fe concentration as well as the isotope ratio of the tracer (^{57}Fe-ferritin), the total Fe concentration in the ferritin standards could be obtained by using the isotope dilution equation.[25]

Quantification of ferritin-bound iron in serum samples

Human serum samples were mixed with an adequate amount of the ^{57}Fe-ferritin tracer and subsequently treated by heat precipitation, aiming at the isolation of serum ferritin. Here, 2 mL of each sample were heated at 75 °C for 10 min. After centrifugation (15 000 *g* for 30 min, 4 °C) the ferritin-containing supernatant was subjected to analysis by SEC-HPLC coupled to DF-ICP-MS.

Results and discussion

Isotopic iron incorporation kinetics

The process of iron incorporation into apo-ferritin takes place in, at least, two steps: (1) oxidation of Fe(II) catalyzed by the H-subunits and (2) translocation and storage of Fe(III) by hydrolysis and polymerization in the central cavity. According to the literature, the H-chains of the ferritin show ferroxidase activity catalyzing the conversion of Fe(II) to Fe(III) which is an initial step in the preparation of iron for storage in the protein. It has been proposed by other authors that the presence of other

ferroxidases such as ceruloplasmin (a serum copper ferroxidase) promotes the incorporation of iron into apoferritin.[26] In this case, Fe(II) seems to bind to the catalytic sites of apoferritin (which might include carboxylate groups) initiating the oxidation process catalysed by the apo-protein. The location of these binding sites has not been determined, but suggested regions are the outer surface of the apoprotein, in the channels leading to the central cavity, or inside the central core. Fig. 1 shows the Fe incorporation kinetics using Mohr's salt as a most stable source of Fe(II): the initial complex formation rate is fast while after some minutes (which differs depending on the Fe(II) concentration) the reaction rate slows down (less apo-protein is available). Such results corroborate that the Fe incorporation into ferritin occurs through a first Fe(II) oxidation step that is catalyzed by apo-ferritin.[26] However, once the concentration of free apo-ferritin decreases, the formation rate of Fe-ferritin is significantly reduced although the complex saturation is not reached even after 30 minutes of reaction time. For practical considerations, this time has been selected as incubation time for further experiments.

To address the purity of the synthesized species, the reaction products were chromatographically separated using size exclusion chromatography with UV/VIS detection and compared with a commercial standard of Fe-containing horse spleen ferritin. These chromatograms can be observed in Fig. 2A and B respectively by monitoring the signals at 280 and 380 nm. These results show that the synthesis product resulted in a main species absorbing at both wavelengths at approximately 11.5 mL, and with a similar retention time to that observed for the commercial Fe-containing horse spleen ferritin. Fig. 2A shows also an iron peak at about 8 mL corresponding to the void volume of the column (species with higher molecular mass than the exclusion limit of the column which is 1300 kDa). This particular species is also detectable in the chromatogram of Fig. 2B of the commercial standard but with a significantly smaller area. A possible explanation for such larger species is

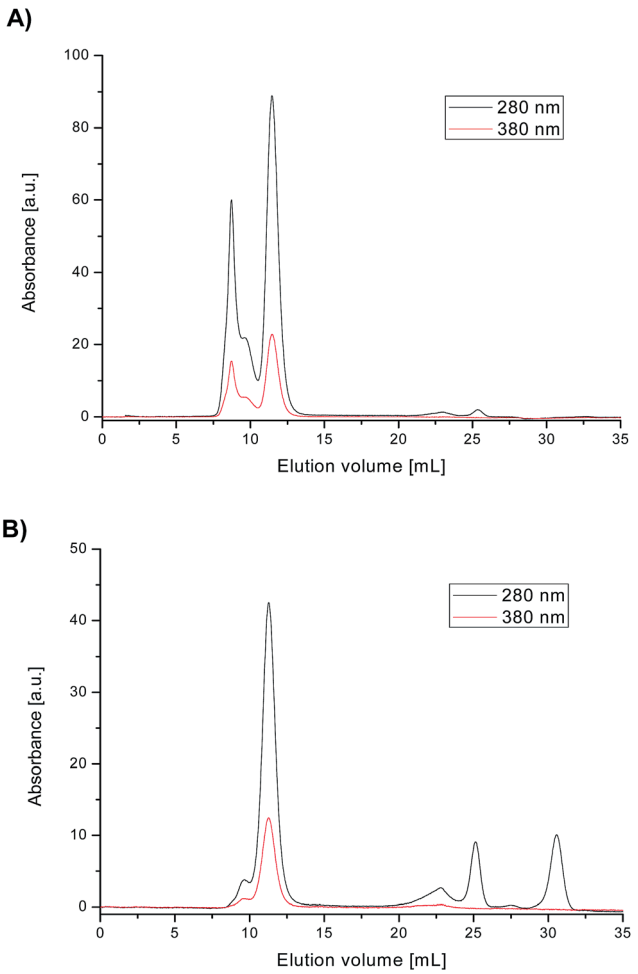

Fig. 2 (A) Size exclusion chromatogram of the reaction products of the incubation of apo-ferritin with $(NH_4)_2{}^{57}Fe(II)(SO_4)_2$ using UV/VIS detection (monitoring the signals at 280 and 380 nm) and (B) chromatogram of the commercial standard of Fe-containing ferritin from horse spleen using the same column.

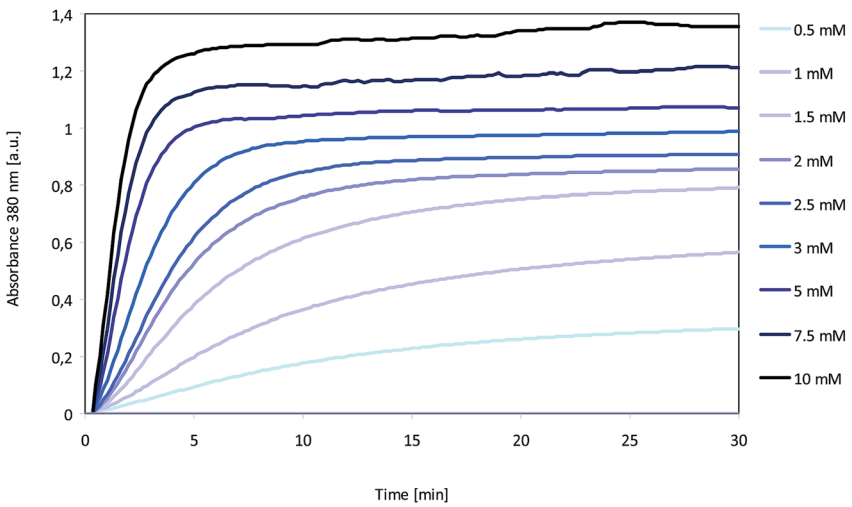

Fig. 1 Incorporation kinetics using 1 μM apo-ferritin solution incubated with 0 to 10 mM of $(NH_4)_2{}^{57}Fe(II)(SO_4)_2$ as a Fe(II) source. The variation of the absorbance detected at 380 nm.

the formation of ferritin dimers, trimers or even oligomers during the synthesis or purification procedures. Such species absorb at the same wavelengths as the monomeric form of ferritin but should behave in a different way in solution (*e.g.* regarding ultrafiltration, antibody recognition, *etc.*). Therefore, the synthesis conducted in this way does not provide a suitable isotopically enriched ferritin standard for further robust quantitative metabolic studies. Thus, specific studies to remove or minimize the formation of oligomers were undertaken.

Oligomerization studies by SEC-UV/VIS and SEC-ICP-MS

In order to study the oligomerization of the ferritin during Fe loading, some initial studies were carried out to address the evolution of the synthesis product with time. The existing literature in this regard is scarce but some papers have reported that the formation of ferritin oligomers can be ascribed to the reduction of disulphide bonds present on the surface of the protein monomers (while Fe(II) converts to Fe(III)).[27] The reactive thiol groups formed in this reduction would undergo subsequent S–S bridging (between several monomers) generating oligomeric ferritin structures. The formation of oligomeric structures was observed during the synthesis and increased by two-fold in just three hours (see ESI†).

Thus, in order to convert the ferritin oligomers into monomers, the originally synthesized product (see Fig. 3A) was treated with powerful reducing agents such as DTT (some authors have reported that the effectiveness of this reagent is dependent on its concentration[20] in such a way that very high DTT concentrations are required to get a significant conversion of oligomers to monomers). In our experiments 1% DTT treatment (see Fig. 3B) did not produce the expected effect. Thus, the complex was also treated with 7 M guanidinium chloride (pH 3.5) which induces extensive unfolding of the protein and dissociation into subunits.[20] The results obtained indicated that the predominant reconstitution products from the oligomers are similar to ferritin monomers, as can be seen in Fig. 3C. This chromatogram reveals also an important decrease in the sensitivity of the original protein peak (a factor of about 3-fold) which could be ascribed to a partial loss or degradation of the protein along the procedure. Guanidinium hydrochloride is a strong disruptive agent (commonly used for disrupting antigen-antibody binding) and the effect on proteins seems to be different depending on the protein target. Helical peptide studies show that guanidinium can be up to 4-fold more efficient than other reagents like urea when planar amino acid side chains are major contributors to helical stability according to some authors. In contrast, guanidinium is barely more efficient than urea if stabilization is mainly due to salt bridges.[28] However, no other significant species seem to be detected in the chromatogram after ultrafiltration. The guanidinum treated samples were stored for over a month and during this time no apparent modification of the chromatographic profile was obtained (see ESI†). Therefore, this preparation strategy was used for the final isotopically enriched species synthesis as described in the procedure section.

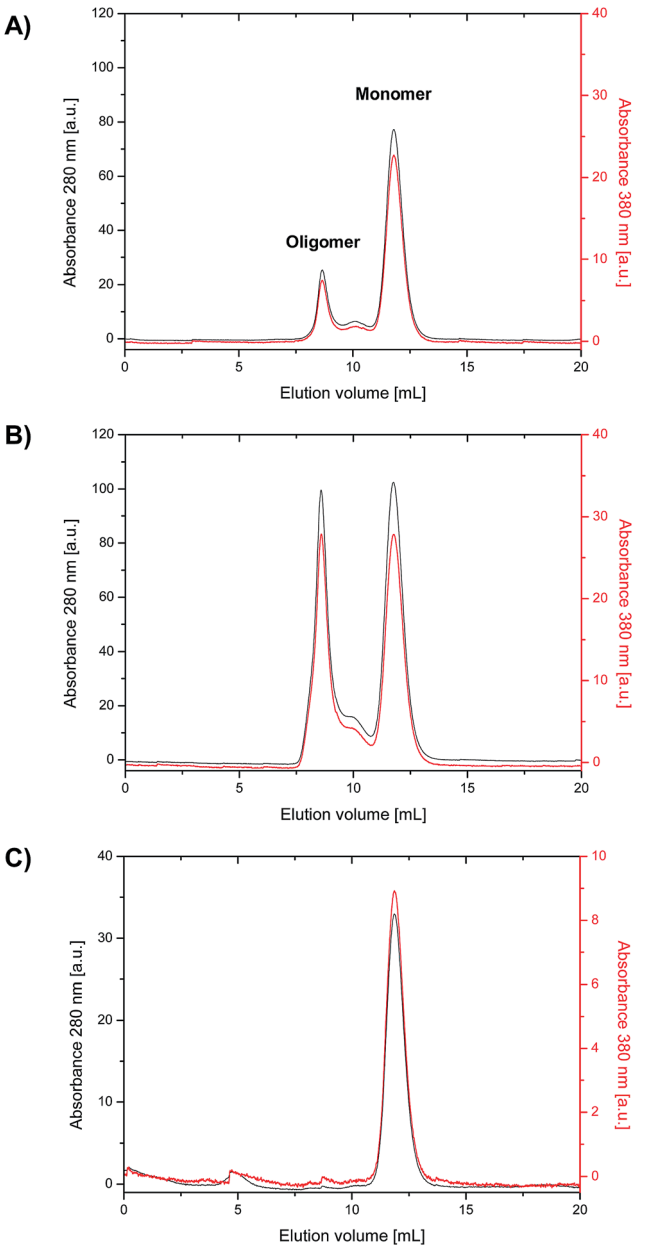

Fig. 3 Chromatograms obtained by UV/Vis detection: (A) directly after apo-ferritin loading with Fe(II) and after the reaction products treated with (B) 1% DTT and (C) 7 M guanidinium chloride (pH 3.5). Monomer eluting at about 11.5 mL and oligomers at 8 mL.

Fig. 4 shows the obtained chromatogram corresponding to the SEC-DF-ICP-MS separation of the isotopically enriched ^{57}Fe-ferritin, monitoring ^{56}Fe and ^{57}Fe. As can be seen, it is possible to address the presence of a pure peak containing mostly ^{57}Fe (blue trace) at the ferritin retention volume of 11.5 mL (comparable to that of the commercial standard containing natural Fe in Fig. 2B). Some other Fe-containing species showing up at 16 minutes, in the black trace, could be ascribed to some impurities present in the commercial apo-ferritin standard and correspond to other Fe-containing proteins (*e.g.* transferrin). This assumption can be supported by the fact that

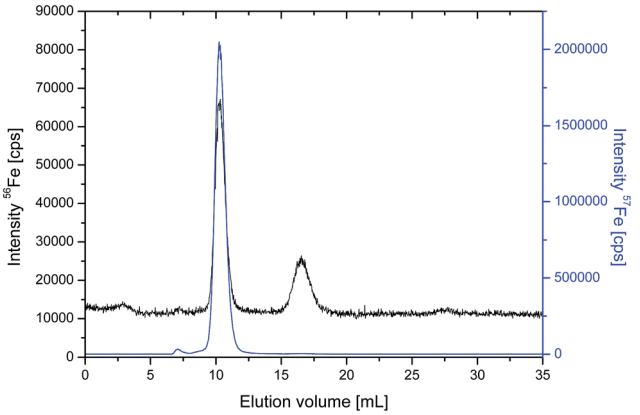

Fig. 4 Chromatogram corresponding to the SEC-DF-ICP-MS separation of the isotopically enriched ^{57}Fe-ferritin complex monitoring ^{56}Fe and ^{57}Fe (black and blue traces, respectively) at about 10.5 mL.

the isotope abundance of this peak corresponds to that of natural Fe and eluted at a different time than the ^{57}Fe-sought species.

Characterization of the ^{57}Fe-ferritin tracer by SEC-ICP-MS and TEM

Once the purity of the isotopically enriched ferritin standard was assessed, the Fe isotopic composition of the enriched complex was calculated by injecting a triplicate of the compound and monitoring all the isotopes (mass bias was taken into account) by MC-ICP-MS. For data treatment, the linear regression slope approach was applied.[29] According to these experiments, relative isotopic abundances of the synthetic ^{57}Fe-ferritin turned out to be: ^{54}Fe 0.08%, ^{56}Fe 3.9%, ^{57}Fe 92.6% and ^{58}Fe 3.5%. These values were similar to the isotopic abundances of the Fe starting enriched material (95% ^{57}Fe) and confirmed that the initial natural Fe present in the apo-ferritin was low while the enrichment level with ^{57}Fe is efficient using Mohr's salt as a stable ^{57}Fe(II) source. In addition to the isotopic abundances, it is necessary to characterize the exact concentration of the tracer in terms of Fe and protein concentration in order to address "the level of iron saturation" of ^{57}Fe-ferritin (meaning, the number of Fe atoms per ferritin molecule). In that vein, a study was conducted by using post-column isotope dilution analysis after SEC separation with ICP-MS detection as described in the procedure section. By taking into account the protein sequence from Swiss Prot database (this is the number of S-containing amino acids per subunit) and measuring the sulphur concentration in the protein using post-column IDA, it is possible to transfer the obtained elemental concentration into ferritin concentration. Simultaneously, standard natural Fe was used for quantification of isotopically enriched ^{57}Fe present in the synthesized standard (by reversed isotope dilution analysis).

The use of post-column IDA for S and Fe determination requires that protein recovery through the column is quantitative. Since recoveries >85% have been obtained in the used column for ferritin standards that requirement is secured. One further consideration is the influence of the occurring H/L chain ratio variations in the ferritin standards with respect to the amino acid composition predicted by the databases. If the differences are very high, this might result in an inaccuracy in the calculation of the ferritin concentration (based on the S-containing amino acids). In order to check for this possibility, a commercial human liver ferritin standard was analyzed simultaneously at different concentrations by its S-content (using S-post column IDA with ICP-MS) as well as by using a previously validated labelling immunoassay.[22] Both sets of experiments (data not shown) provided undistinguishable results (slope of the plotted results 1.02 and correlation coefficient $r^2 = 0.992$) confirming the suitability, in this case, of the proposed approach based on S measurement to address the protein concentration.

The obtained results for the characterization of the ^{57}Fe-ferritin are summarized in Table 2 including protein concentration, Fe concentration and Fe : ferritin ratios. On average, the number of Fe atoms per ferritin turned out to be about 2200 which is in good agreement with the existing literature on this regard. This documents that even when the protein cage can accommodate up to 4500 atoms of Fe, naturally found Fe : ferritin ratios are lower and do not exceed 1500 atoms per molecule of ferritin in liver cells of haemochromatosis patients.[30]

To finally confirm that ^{57}Fe is specifically incorporated into the ferritin cage and not bound unspecifically within the protein, TEM images of the apoferritin, commercial holoferritin and the synthesized ^{57}Fe-ferritin were taken for comparative purposes. Fig. 5 shows all the images together with the histograms corresponding to the mean diameters determined in each case. Thus, mean diameters were 3.8 ± 1.0, 5.80 ± 0.85 and 6.82 ± 0.70 nm for apoferritin, commercial holoferritin and synthesized ^{57}Fe-ferritin. These results corroborate that the synthesis used in this work has successfully accomplished the formation of iron oxide nanoparticles into the core of apoferritin. Additionally, the size of the Fe core seems higher in the synthesized protein than in the case of the commercial holoferritin (5.80 *vs.* 6.82). In order to quantitatively address these differences in terms of the Fe content of the different ferritin forms, the synthesized ^{57}Fe-ferritin was used as a tracer to conduct species specific isotope dilution analysis for the determination of the Fe content in the commercial apo and holoferritin using the methodology we described previously in the literature.[31] Fig. 6 shows the chromatograms obtained for

Table 2 Quantitative results obtained for the analysis of total ferritin, iron in ferritin and Fe : ferritin ratio in the synthesized isotopically enriched ^{57}Fe-ferritin

	Average	SD	%RSD
Fe concentration	2.86 μg mL^{-1}	0.04	1.46
	51.58 nmol mL^{-1}	0.76	
Ferritin concentration	13.5 μg mL^{-1}	1.32	9.8
	23.4 pmol mL^{-1}	2.29	
Fe : Ferritin	2213	185	8.4

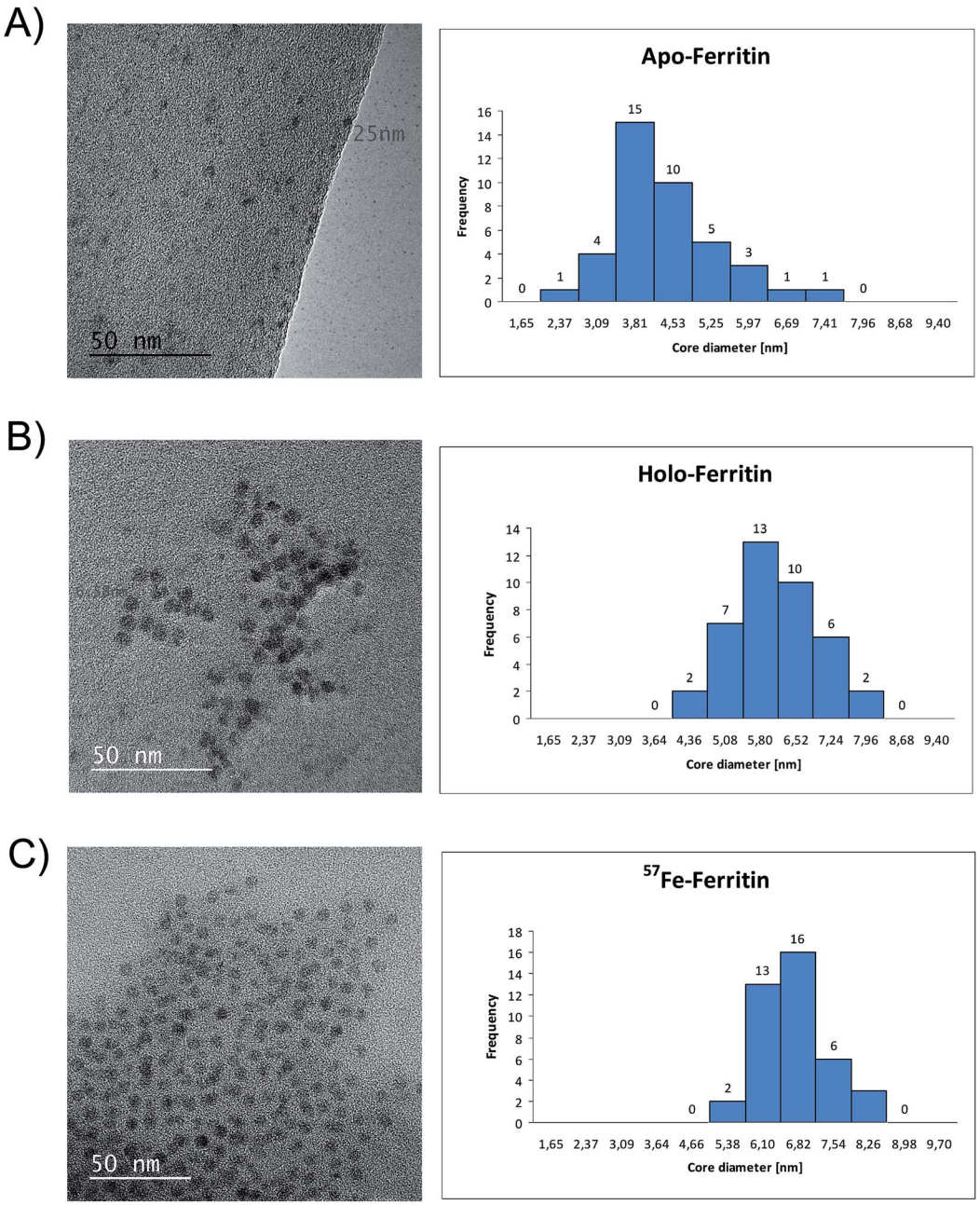

Fig. 5 Images obtained by TEM of the different ferritin molecules from horse spleen together with the histograms of the measured nanoparticle diameters: (A) apoferritin, (B) holoferritin and (C) ^{57}Fe-ferritin synthesized with the proposed methodology.

apoferritin (Fig. 6A, low Fe content) and for holoferritin (Fig. 6B, containing a higher Fe concentration) both from horse spleen after mixing with the synthesized tracer and IDA analysis.

Table 3 shows a summary of the obtained results for these determinations (total protein concentration was calculated by conducting post-column isotope dilution of S as previously described). It can be observed that the Fe : ferritin ratios in the apo-ferritin from horse spleen are very low (about 200) but there is still some Fe present in the protein core, as observed in the TEM image. On the other hand, the Fe : ferritin content in the commercial horse spleen ferritin turned out to be about 1000 atoms per ferritin molecule which is remarkably lower (by a factor of 2-fold) than in the synthesized ferritin and also in agreement with the TEM image (revealing an Fe core of about 5.8) and with the reported values in the literature.[32] In brief, after such characterization results it can be concluded that the synthesized ^{57}Fe-ferritin standard can be used as a nano-metabolic tracer for quantitative studies, for instance, on the Fe release or its incorporation kinetics under different pathological situations and be compared with normal healthy conditions.

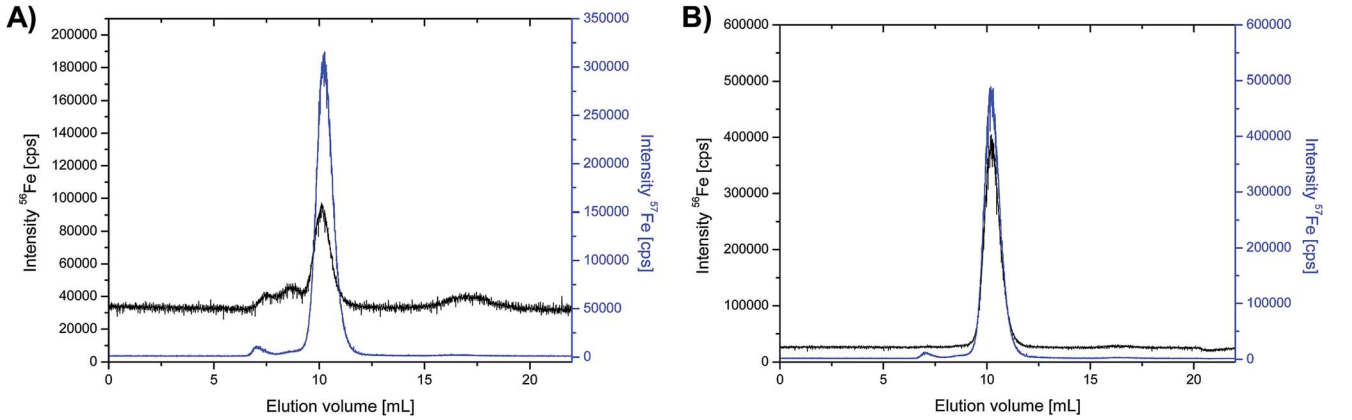

Fig. 6 Size exclusion chromatograms obtained from a mixture of the synthesized isotopically enriched ^{57}Fe-ferritin: (A) apo-ferritin (equine spleen) and (B) human spleen ferritin by using the ^{57}Fe-ferritin tracer by using DF-ICP-MS detection both eluting at about 10.5 mL.

Table 3 Quantitative results obtained for the analysis of total ferritin, iron and Fe : ferritin ratios in the quantified commercially available ferritin standards

	Horse-spleen ($n = 3$)	Apo-ferritin
Fe concentration	1.47 ppm 26.2 μmol L^{-1}	6.7 ppm 119.5 μmol L^{-1}
Ferritin concentration	14.3 ppm 26.2 nmol L^{-1}	311.7 ppm 623.2 nmol L^{-1}
Fe : Ferritin	1030 ± 20	190

Determination of Fe : ferritin ratios in serum samples

The labeled ferritin was applied for the quantification of ferritin-bound iron in different human serum samples ($n = 8$) as described in the procedure section. In Table 4 the determined ferritin-bound iron concentrations are represented. Here, a mean concentration of 12.35 ± 6.99 ng g^{-1} ferritin-bound iron was determined which is in excellent agreement with previously obtained results using post column IDA after protein purification.[24] To address the serum ferritin concentration, each serum sample was analyzed by ECLIA enabling the calculation of the Fe : ferritin ratios. The obtained Fe : ferritin ratios indicate a correlation between low serum ferritin concentration (<75 ng mL^{-1}) and higher Fe : ferritin ratios, similar to what was observed in the previous experiments with this kind of samples. However, the developed protocol enables the absolute determination of ferritin-bound iron in human serum samples with the advantage that once the spike and the sample are mixed, all further sample losses are compensated (such losses accounted for almost 70% as previously described).[24] Consequently, no sample recoveries during purification or chromatographic separation have to be taken into account.

Table 4 Quantitative results obtained for the analysis of total ferritin, iron and Fe : ferritin ratios in serum samples from patients containing ferritin levels below 75 ng mL^{-1}

Fe (SEC-DF-ICP-MS)		Ferritin (ECLIA)		
ng g^{-1}	nmol g^{-1}	ng mL^{-1}	fmol mL^{-1}	Fe : Ferritin
2.65	0.05	9	17.18	2766
11.17	0.20	73	139.37	1436
12.16	0.22	33	63.01	3456
12.23	0.22	27	51.55	4249
15.99	0.29	60	114.55	2500
17.45	0.31	54	103.10	3031
23.66	0.42	67	127.92	3312

Conclusions

The chemical incorporation of Fe(II) from dissolved $(NH_4)_2Fe(II)(SO_4)_2$ into apo-ferritin has been proved to follow a first order reaction kinetics catalyzed by apo-ferritin. Importantly, during the Fe(II) incorporation into the protein the formation of ferritin oligomers was observed. To disrupt such aggregates, 7 M guanidinium hydrochloride (pH 3.5) produced satisfactory results and showed that the interactions to form oligomers are relatively strong. The studied and optimized synthesis was then conducted with isotopically enriched $(NH_4)_2{}^{57}Fe(II)(SO_4)_2$ and the resulting isotopically enriched protein turned out to provide Fe : ferritin ratios of about 2200 Fe atoms per ferritin molecule and about ^{57}Fe 92.6% isotopic abundances as obtained by MC-ICP-MS.

The complementary information about NP size provided by the TEM measurement in the same standards revealed first that ^{57}Fe is incorporated specifically within the protein core in the form of an iron oxide nanoparticle with a final diameter of about 6.8 nm; second, the use of the synthesized nanotracer of ^{57}Fe-ferritin by SEC-ICP-MS provided important information on the saturation level of the commercial horse spleen ferritin in the apo and holo forms and their correlation with the inner protein core size variation obtained by TEM. Therefore, the developed enriched standard together with the optimized methodology has been applied to address Fe : ferritin ratios in important biological samples (*e.g.* serum) and will be applied in other samples to understand a bit further the implication of ferritin and iron uptake in health and disease

(*e.g.* hyperferritinemia which may be associated with iron overload, inflammation or even cancer).[33] In addition, the proposed strategy could have a great impact to investigate in depth the efficacy of new Fe-pharmaceutical preparation methods to combat Fe deficiencies (*e.g.* those using Fe-nanoparticles, recently applied to treat severe anaemia).[34]

Acknowledgements

The authors would like to thank Prof. Santiago García-Granda for his help on the X-ray characterization of the synthesized Mohr's salt and Prof. Nacho Garcia Alonso for the help with the MC-ICP-MS experiments. The financial support from MICINN through the FPU grant AP2008-04449 of T. Konz and through the projects CTQ2006-02309 and CTQ2011-23038 is gratefully acknowledged.

References

1 M. Wessling-Resnick, *Annu. Rev. Nutr.*, 2000, **20**, 129–151.
2 N. C. Andrews, *N. Engl. J. Med.*, 1999, **341**, 718–724.
3 M. Muñoz, J. A. García-Erce and A. F. Remacha, *J. Clin. Pathol.*, 2011, **64**, 287–296.
4 H. A. Huebers, M. J. Eng, B. M. Josephson, N. Ekpoom, R. L. Rettmer, R. F. Labbé, P. Pootrakul and C. A. Finch, *Clin. Chem.*, 1987, **33**, 273–277.
5 M. E. Del Castillo Busto, M. Montes-Bayón, J. Bettmer and A. Sanz-Medel, *Analyst*, 2008, **133**, 379–384.
6 M. A. Knovich, J. A. Storey, L. G. Coffman, S. V. Torti and F. M. Torti, *Blood Rev.*, 2009, **23**, 95–104.
7 E. C. Theil, *J. Nutr.*, 2003, **133**, 1549S–1553S.
8 S. Ferraro, R. Mozzi and M. Panteghini, *Clin. Chem. Lab. Med.*, 2012, **50**, 1911–1916.
9 F. Carmona, O. Palácios, N. Gálveza, R. Cuesta, S. Atriand, M. Capdevila and J. M. Domínguez-Vera, *Coord. Chem. Rev.*, 2013, **257**, 2752–2764.
10 S. Stanley, *Curr. Opin. Biotechnol.*, 2014, **28**, 69–74.
11 N. D. Chasteen and P. M. Harrison, *J. Struct. Biol.*, 1999, **126**, 182–194.
12 M. Wagstaff, M. Worwood and A. Jacobs, *Biochem. J.*, 1978, **173**, 969–977.
13 L. Zecca, M. B. H. Youdim, P. Riederer, J. R. Connor and R. R. Crichton, *Nat. Rev. Neurosci.*, 2004, **5**, 863–873.
14 Y. Ke and Z. M. Qian, *Lancet Neurol.*, 2003, **2**, 243–253.
15 D. B. Kell and E. Pretorius, *Metallomics*, 2014, **26**, 748–773.
16 M. Hoppler, L. Meile and T. Walczyk, *Anal. Bioanal. Chem.*, 2008, **390**, 53–59.
17 M. Hoppler, C. Zeder and T. Walczyk, *Anal. Chem.*, 2009, **81**, 7368–7372.
18 J. A. Rodríguez-Castrillón, M. Moldovan, J. I. García Alonso, J. J. Lucena, M. L. García-Tomé and L. Hernández-Apaolaz, *Anal. Bioanal. Chem.*, 2008, **390**, 579–590.
19 D. De Silva, D. M. Miller, D. W. Reif and S. D. Arch, *Biochem. Biophys.*, 1992, **293**, 409–415.
20 Y. Niitsu and I. Listowsky, *Biochemistry*, 1973, **12**, 4690–4694.
21 M. Wang, W. Feng, W. Lu, B. Li, B. Wang, M. Zhu, Y. Wang, H. Yuan, Y. Zhao and Z. Chai, *Anal. Chem.*, 2007, **79**, 9128–9134.
22 C. Rappel and D. Schaumlöffel, *Anal. Bioanal. Chem.*, 2008, **390**, 605–615.
23 N. Zinn, R. Krüger, P. Leonhard and J. Bettmer, *Anal. Bioanal. Chem.*, 2008, **391**, 537–543.
24 T. Konz, E. Añón-Alvarez, M. Montes-Bayon and A. Sanz-Medel, *Anal. Chem.*, 2013, **85**, 8334–8340.
25 K. G. Heumann, L. Rottmann and J. Vogl, *J. Anal. At. Spectrom.*, 1994, **9**, 1351–1355.
26 G. R. Bakker and R. F. Boyer, *J. Biol. Chem.*, 1986, **261**, 13182–13185.
27 M. Wagstaff, M. Worwood and A. Jacobs, *Biochem. J.*, 1978, **173**, 969–77.
28 W. K. Lim, J. Rosgen and S. W. Englander, *Proc. Natl. Acad. Sci. U. S. A.*, 2009, **106**, 2595.
29 V. N. Epov, S. Berail, M. Jimenez-Moreno, V. Perrot, C. Pecheyran, D. Amouroux and O. F. X. Donard, *Anal. Chem.*, 2010, **82**, 5652–5662.
30 Y. H. Pan, K. Sader, J. J. Powell, A. Bleloch, M. Gass, J. Trinick, A. Warley, A. Li, R. Brydson and A. Brown, *J. Struct. Biol.*, 2009, **166**, 22–31.
31 M. E. Del Castillo Busto, M. Montes-Bayon and A. Sanz-Medel, *Anal. Chem.*, 2006, **78**, 8218–8226.
32 S. Gider, D. Awschalom, T. Douglas, S. Mann and M. Chaparala, *Science*, 1995, **268**, 77–80.
33 S. I. Shpyleva, V. P. Tryndyak, O. Kovalchuk, A. Starlard-Davenport, V. F. Chekhun, F. A. Beland and I. P. Pogribny, *Breast Cancer Res. Treat.*, 2011, **126**, 63–71.
34 M. R. Jahn, H. B. Andreasen, S. Fütterer, T. Nawroth, V. Schünemann, U. Kolb, W. Hofmeister, M. Muñoz, K. Bock, M. Meldel and P. Lagguth, *Eur. J. Pharm. Biopharm.*, 2011, **78**, 480–491.